



Structural and magnetic properties of MgFe_2O_4 nanopowder synthesized via co-precipitation route

Farhana Naaz¹ · Hemant Kumar Dubey¹ · Chanda Kumari¹ · Preeti Lahiri¹ Received: 16 January 2020 / Accepted: 26 March 2020 / Published online: 3 April 2020
© Springer Nature Switzerland AG 2020

Abstract

Mg ferrite was successfully synthesized by adopting a simple co-precipitation route. A physical property of Mg ferrite has been investigated employing XRD, FTIR, SEM, EDS, AFM and Raman spectroscopic techniques. The XRD results indicated the formation of single phase spinel ferrite with crystalline size of 36 nm. FTIR results confirmed ferrite tetrahedral (580 cm^{-1}) and octahedral sites (430 cm^{-1}) metal oxygen vibrations. The Raman result revealed the well defined Raman active modes of synthesized sample. Scanning electron microscopic (SEM) studies revealed nano crystalline nature of the sample. An elemental composition of the sample was studied by energy dispersive spectroscopy (EDS). Crystallite size, X-ray density, hopping length, and magnetic properties of the product are also reported. AFM provides surface roughness. The magnetic hysteresis curves clearly indicate the soft nature of the prepared nanoferrite. The Raman spectra shows five Raman active modes ($A_{1g} + E_g + 3F_{2g}$) which are expected in the spinel structure and Raman spectra has a very good agreement with reported data. Various magnetic parameters such as saturation magnetization (M_s), and remanence (M_r) and coercivity (H_c) are obtained from the hysteresis loops.

Keywords Nanoparticles · XRD · Ferrite · Raman spectra · Magnetism

1 Introduction

Nanoparticles of spinel ferrite draw significant consideration due to their lower density and higher specific surface area and distinct optical, catalytic and magnetic properties [1]. Study of spinel ferrite MFe_2O_4 (where M = metal ion) nanoparticles has significant application in modern technologies such as contrast enhancement of magnetic resonance imaging, high density data storage, and magnetic carriers for site-specific drugs delivery [2]. Spinel ferrites have the general molecular formula MFe_2O_4 where M^{2+} and Fe^{3+} are the divalent and trivalent cations occupying tetrahedral (A) and octahedral (B) interstitial positions of the FCC lattice formed by O^{2-} ions. Among the spinel ferrites, MFe_2O_4 nanoparticles finds extensive applications in magnetic based diagnosis and treatment

devices [3], potential magnetorheological fluids [4], gas sensors [5], catalysts [6], and lithium ion batteries [7]. Magnesium ferrite is a soft magnetic n-type semiconducting material [8, 9]. Recent increasing attention to nanostructures of magnetic materials has been due to their unique material properties that are significantly different from those of their bulk counter parts [10, 11]. Physical, chemical and structural properties of oxide powders depend on preparation method and thermal treatment applied during preparation. A wide variety of methods are being used to synthesize spinel ferrite nanoparticles including citric acid combustion [12], sol-gel auto combustion [13], hydrothermal [14], co-precipitation methods [15, 16]. In addition, thermolysis [17], wet chemical co-precipitation technique [18], self-propagating and microemulsion [19, 20], are also used. The experimental conditions used in the

✉ Preeti Lahiri, plahiri16@yahoo.com | ¹Department of Chemistry, Mahila Mahavidyalaya, Banaras Hindu University, Varanasi 221005, U.P, India.



preparation of these materials play an essential role in the properties and the particle size of the ferrite nanoparticles produced. Co-precipitation method is one of the promising techniques for preparing nano ferrites in bulk scale due to the production of homogeneous particles. Co-precipitation synthesis involves dissolution of compound salt precursor in aqueous media and subsequent precipitation from the solution by pH adjustment. It is a useful method for the preparation of ceramics and metal oxide powders.

For MgFe_2O_4 nanoparticles, many researchers reported [21–24] on their nanostructures and properties. Sivakumar et al. [23], obtained nanocrystalline MgFe_2O_4 with grain size of 19–72 nm using ceramic method. It was observed that the sample with a grain size of 72 nm got the highest saturation magnetization of 36 emu g^{-1} at 293 K. Hankare et al. [24] synthesized polycrystalline magnesium ferrite by co-precipitation method and measured its gas-sensation. The electrical properties and sensing properties towards carbon dioxide of MgFe_2O_4 powder were studied by Sumangala et al. [25]. Nanoparticles of MgFe_2O_4 have good photoelectrical properties [26]. Properties of ferrite materials are strongly influenced by the distribution of metallic ions among crystallographic lattice sites which in turn are sensitive to the synthetic method employed.

In the present investigation, we report the structural and physicochemical properties of magnesium ferrite MgFe_2O_4 nanoparticles by using various different characterization parameters like XRD, FT-IR, SEM, EDS and magnetic. Raman spectroscopic studies which is powerful probe to reveal the vibrational and structural properties of the materials was also employed. Moreover, AFM was included to understand the surface roughness of the nanoparticles as a little information is available for the surface properties in the literature.

In the present investigation, we report the structural and physicochemical properties of magnesium ferrite nanoparticles prepared by using co-precipitation technique.

2 Experimental

2.1 Synthesis

In this study, sample with a formula MgFe_2O_4 was synthesized by wet chemical co-precipitation technique. An aqueous precursor solution was prepared by dissolving 6.460 g $\text{Fe}(\text{NO}_3)_3 \cdot 9\text{H}_2\text{O}$, and 2.102 g $\text{Mg}(\text{NO}_3)_2 \cdot 4\text{H}_2\text{O}$ into 100 ml double distilled water. Sodium hydroxide (0.1 M) was dropped in the salt solution drop wise for 40 min at the constant temperature of 80°C with vigorous stirring on magnetic stirrer. The pH of the solution was adjusted to be 10. Digestion was performed for 90 min. Particles were settled down at the bottom of the beaker. It was filtered

and washed repeatedly with distilled water. The residue was dried at 100°C for 4 h, and subsequently calcined at 500°C for 3 h to get dark brown ferrites as end product.

2.2 Characterization

Synthesized sample of magnesium ferrite nanoparticles was subjected to various techniques for structural investigations as described below. The crystal structure was studied by using X-ray diffraction (XRD) (Rigaku Miniflex 600, Japan) technique with Cu-K α radiation at 40 keV for phase determination of sample. FT-IR spectra were recorded by employing Perkin Elmer spectrophotometer in $400\text{--}4000 \text{ cm}^{-1}$ range to confirm metal oxide bonding present in materials. The surface morphology of the sample and elemental analysis were performed by using Scanning Electron Microscopy (SEM) (ZEISS, model EVO-18 research, Germany) equipped with an Energy Dispersive X-ray Analyser (EDX, Oxford instrument USA). Surface roughness was determined by Atomic force Microscopy (AFM) (model NTEGRA PRIMA, NT-MDT, Russia). Raman spectra was performed using the model RENISHAW In-VIA Raman microscope to identify frequency modes of tetrahedral and octahedral sites. The magnetic properties of the calcined powder (500°C) have been investigated by vibrating sample magnetometer using SQUID based magnetometer (MPMS 3).

3 Results and discussion

3.1 X-ray diffraction studies

X-ray diffraction study was performed to identify the phase formation of the prepared ferrite materials. Figure 1 shows the indexed x-ray diffraction patterns of the synthesized sample of MgFe_2O_4 using chemical co-precipitation technique. The presence of planes (111), (220), (311), (400), (422), (511), (440), (533), (622), (444) confirm the formation of cubic spinel structure. The data were collected at 2θ range from 20 to 80 degree. The diffraction peaks are in agreement with the international standard diffraction data card JCPDS number 89–3084. Lattice parameter, cell volume, crystallite size (D) and XRD density were estimated for ferrite nano powder and included in the Table 1. The crystallite size (D) of MgFe_2O_4 sample was calculated from X-ray diffraction line broadening of (311) peak using the Scherrer equation [27];

$$D = k\lambda/\beta \cos \theta$$

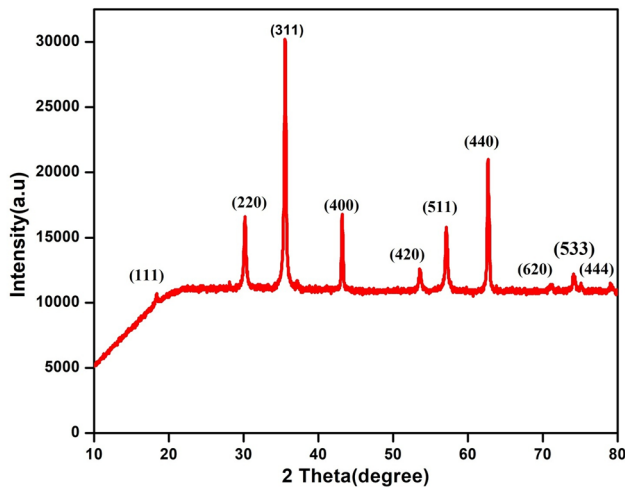


Fig. 1 Indexed X-ray diffraction pattern of magnesium ferrite nanoparticles synthesized by wet chemical co-precipitation technique

where k is constant and taken as 0.91, λ is the wavelength ($\lambda = 1.5406 \text{ \AA}$) of X-ray beam used, β is the full width at half maximum (FWHM) of diffraction peak at an angle θ . The (311) peak has been chosen for calculation as the most intense peak. Theoretical density (ρ_x) was evaluated by the following formula [28];

$$\rho_x = 8M/N a^3$$

where M , a , N are molar mass, lattice parameter and Avogadro's number respectively. Density of ferrite sample was found to be 4.5306 g/cm^3 . Lattice parameter (a) was calculated by the following relationship;

$$a = d (h^2 + k^2 + l^2)^{1/2}$$

where d is diffracting plane spacing and h , k , l miller indices of the diffracting plane. Unit cell volume was evaluated from the following relation;

$$V = a^3, \text{ in } \text{\AA}^3 \text{ unit}$$

and its value was obtained as 586.37 \AA^3 and included in the Table 1. Lattice constant obtained using the XRD data is found to be 8.37 \AA (Table 1) which is in good agreement with the reported value. The crystallite size of the sample was obtained 36.6 nm . The distance between.

magnetic ions hopping length in A sites (tetrahedral) and B sites (octahedral) were calculated by using relations [29];

$$d_A = 0.25a$$

$$d_B = 0.25a$$

The values of hopping lengths (Table 1) for two sites were found to be 3.624 \AA and 2.958 \AA respectively.

3.2 Fourier Transform Infrared analysis

FTIR spectrum of MgFe_2O_4 ferrite prepared by co-precipitation method was shown in Fig. 2. FTIR analysis confirms the formation of spinel structure of ferrites. FTIR spectroscopy reveals the cation and anions distribution on octahedral and tetrahedral lattice sites. We observed two ranges of absorption bands in spinel ferrite MgFe_2O_4 , the higher frequency band (ν_1) lies in 580 cm^{-1} and low frequency band (ν_2) lies in the 430 cm^{-1} . In spinel ferrites, the high frequency bands around 600 cm^{-1} is due to stretching intrinsic vibration of unit cell of spinel in tetrahedral sites (A) and lower frequency band around 400 cm^{-1} is due to stretching vibration of metal oxygen in octahedral sites (B) [30]. This is due to shorter bond length of metal oxygen of tetrahedral sites and longer bond length of metal

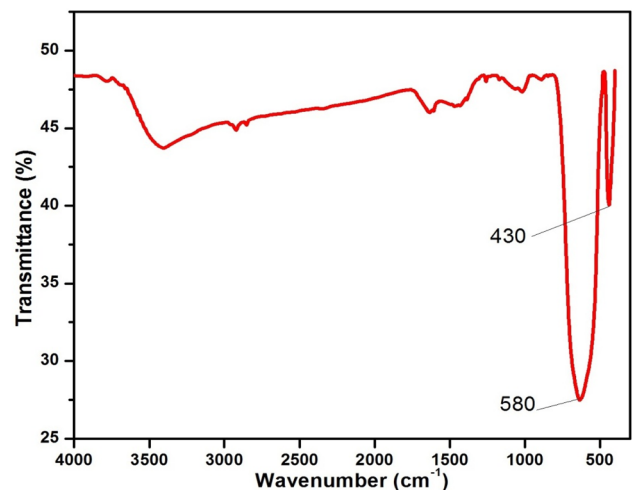


Fig. 2 FTIR spectra of magnesium ferrite nanoparticles synthesized using wet chemical co-precipitation technique

Table 1. Values of crystallite size, lattice parameter (a), unit cell volume, theoretical density and hopping length for A-Site (d_A) and B-Site (d_B) of Mg Nano ferrite

Lattice parameter $a (\text{\AA})$	Crystallite size $D (\text{nm})$	Theoretical density $\rho_x (\text{g/cm}^3)$	Unit cell volume $V (\text{\AA}^3)$	Force constant $K_t \times 10^5$ (dyne/cm)	Force constant $K_o \times 10^5$ (dyne/cm)	A site $d_A (\text{\AA})$	B Site $d_B (\text{\AA})$
8.3712	36.6	4.5306	586.60	2.446	1.344	3.6242	2.9587

oxygen in octahedral sites. The band which is present in 1600 cm^{-1} to 3400 cm^{-1} represents stretching and bending vibrations of O–H which shows the free and absorbed water in sample.

3.3 Surface morphological studies

Scanning electron microscopy (SEM) was carried out to observe the morphology of the synthesized product. Figure 3 shows the 200 nm scale morphology of Mg-ferrite powder calcinated at $500\text{ }^\circ\text{C}$. The observed SEM images clearly revealed that the magnetic ferrite particles are formed with some agglomeration at nanoscale. Figure 3 shows characteristic SEM image of MgFe_2O_4 . Microstructure analysis determines the average size and the type of grain growth of the sample, which influences the physical, electrical and magnetic properties of the materials. The particles have homogenous distribution. Agglomeration was also observed as small particles aggregated in order to achieve lower free energy state. Figure 4 shows the energy dispersive spectrum (EDS) for MgFe_2O_4 powder and Table 2 gives quantitative estimation of elements obtained directly from spectrum through its atomic and weight percentages and corresponding theoretical values. The results confirmed the presence of the required elements in the prepared composition with almost all the peaks associated with elements such as those of Mg, Fe, O, thereby suggesting the formation of pure MgFe_2O_4 .

Atomic force microscopy is one of the important spectroscopic techniques for surface analysis because of high resolution and powerful analysis software. The visualization of AFM is three dimensions and it widely visualizes individual particles and group of particles. Figure 5a,

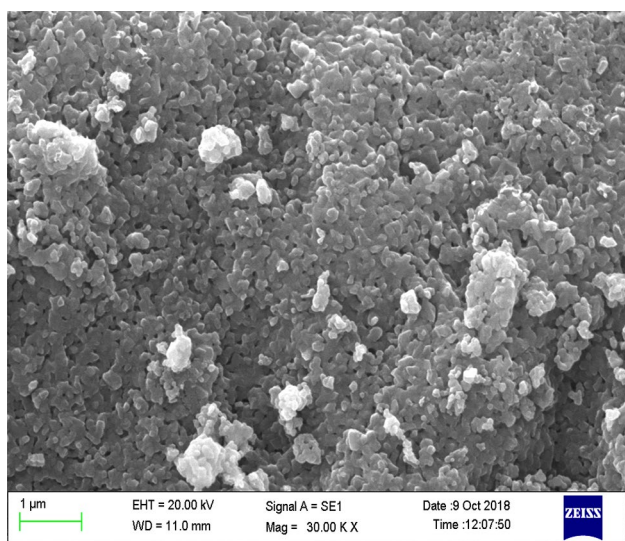


Fig. 3 SEM micrograph of MgFe_2O_4 powder

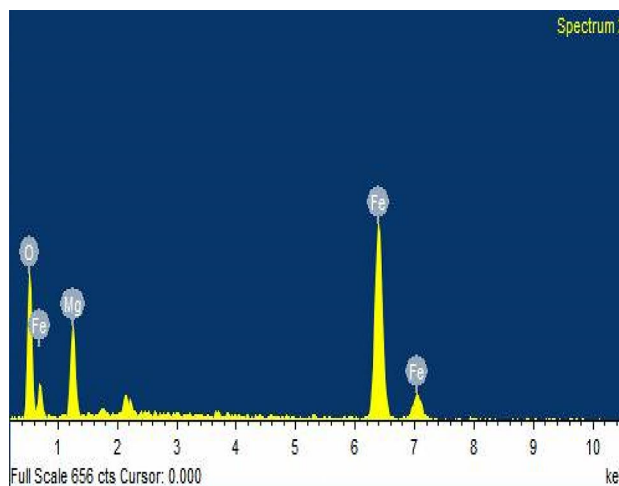


Fig. 4 EDS spectra of MgFe_2O_4 powder

b show the two and three dimensional AFM images of MgFe_2O_4 respectively and their corresponding histogram and size distribution are displayed in Fig. 5c, d. The roughness of thin film is characterized by the root mean square (RMS) and average roughness (R_q) and corresponding experimental values of RMS and R_q obtained as 4.824 nm and 3.640 nm respectively. The structure consists of small round granules. The maximum height (R_p) is 37.93 nm and a maximum depth (R_v) is 17.04 nm respectively.

3.4 Raman studies

Raman spectra were recorded at room temperature for MgFe_2O_4 nano powder. MgFe_2O_4 spinel has a cubic structure belonging to the space group $Fd3m$. Although the full unit cell contains 56 atoms ($Z=8$), the smallest Bravais cell only contains 14 atoms ($Z=2$). As a result, the factor group analysis predicts the following modes in MgFe_2O_4 spinel:

$$A_{1g}(R) + E_g(R) + F_{1g} + 3F_{2g}(R) + 2A_{2u} + 2E_u + 4F_{1u}(IR) + 2F_{2u}$$

There are five Raman active modes ($A_{1g} + E_g + 3F_{2g}$), composed of the motion of O ions and both the A-site and

Table 2. Experimental values obtained from the spectrum of energy dispersive X-ray analysis for various constituent elements present in magnesium ferrite

Element	Experimental values		Theoretical value	
	Weight %	Atomic %	Weight %	Atomic %
O	28.17	52.58	31.98	57.15
Mg	12.99	15.96	12.15	14.26
Fe	58.84	31.46	55.84	28.57
Total	100.0			

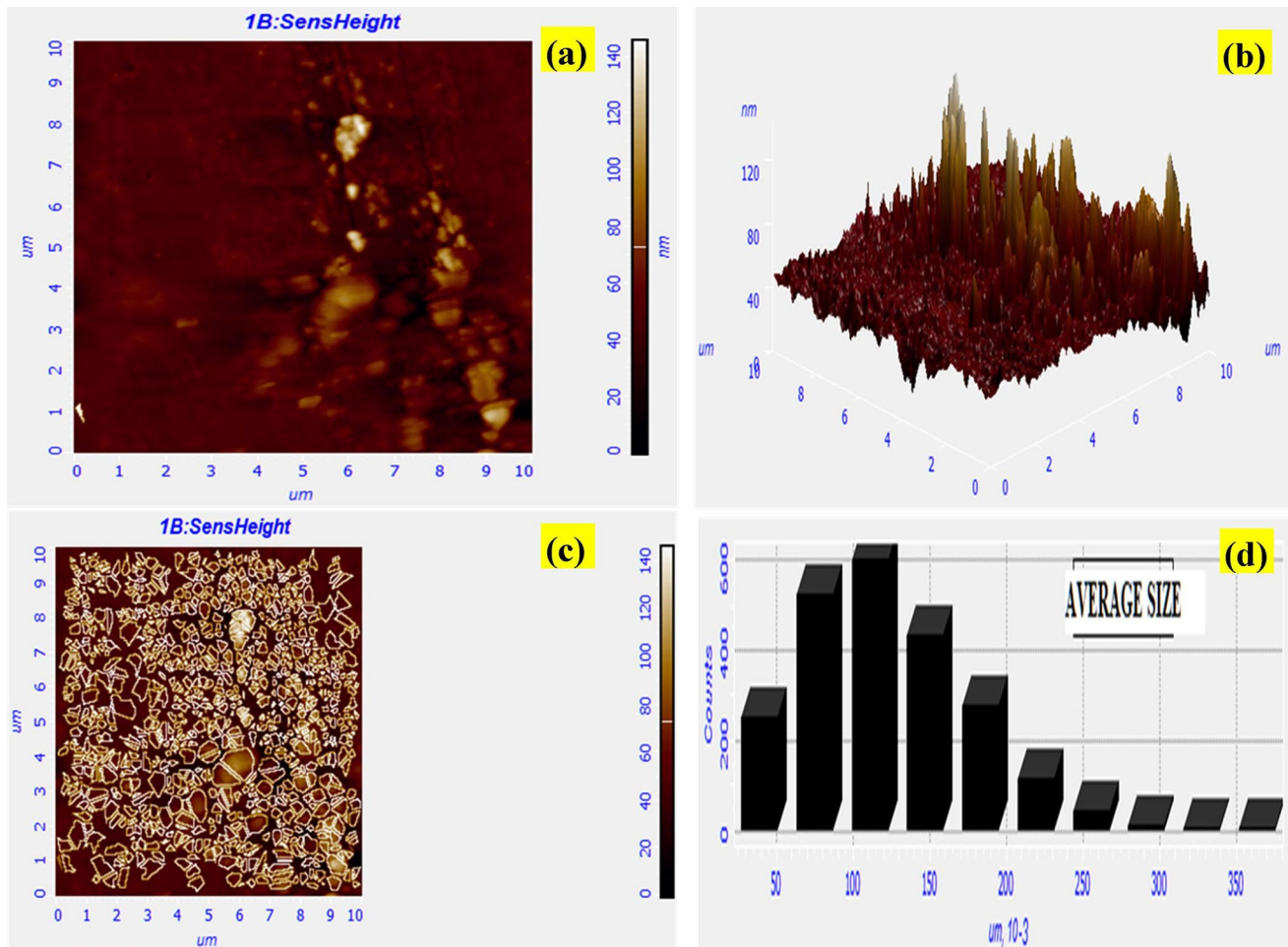


Fig. 5 AFM images of MgFe_2O_4 nanoparticles at room temperature. **a** Two dimensional, **b** three dimensional images, **c** grain size analysis and **d** histogram

B-site ions [31, 32]. Generally, in ferrites, the modes above 600 cm^{-1} belong to the motion of the oxygen atoms in tetrahedral AO_4 group and modes below 600 cm^{-1} belong to the motion of the oxygen atoms in octahedral BO_6 [33]. Figure 6 shows the room-temperature Raman spectra of the MgFe_2O_4 . The spectra consist of all five Raman modes at 217, 329, 480, 548 and 704 cm^{-1} (given in the Table 3) which are in good agreement with the literature report [34].

The A_{1g} mode is due to symmetric stretching of oxygen atoms along metal–oxygen bonds in the tetrahedral coordination. E_g is due to symmetric bending of oxygen with respect to the metal ion in AO_4 unit and $F_{2g}(3)$ is caused by asymmetric bending of oxygen. $F_{2g}(2)$ is due to asymmetric stretching of metal and oxygen. $F_{2g}(2)$ and $F_{2g}(3)$ correspond to the vibrations of octahedral group. $F_{2g}(1)$ is due to translational movement of the tetrahedron (metal ion at tetrahedral site together with four oxygen atoms). In the present study, five observed Raman modes (Table 3)

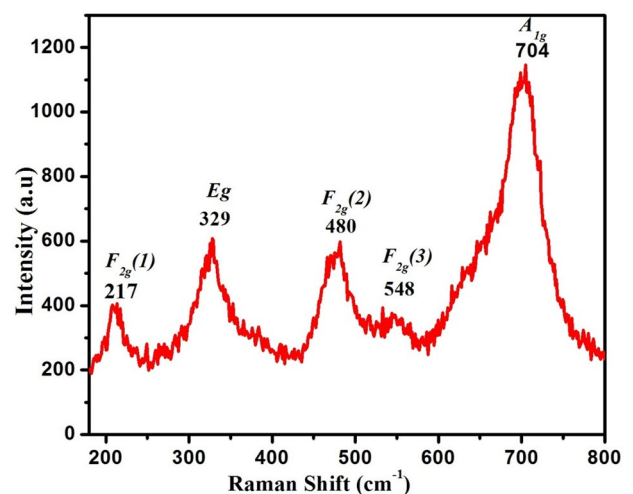
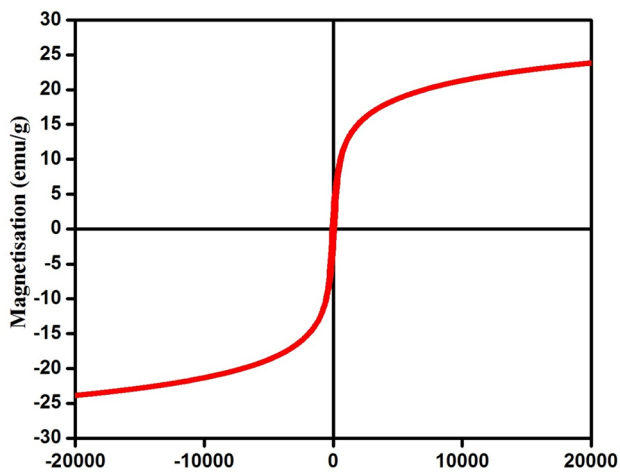


Fig. 6 Room temperature Raman scattering spectra of MgFe_2O_4 sample

Table 3. Assignments for Raman modes in the spinel MgFe_2O_4 observed at room temperature

Raman modes (cm^{-1})	Assignment
217	F_{2g} (1)
329	E_g
480	F_{2g} (2)
548	F_{2g} (3)
704	A_{1g}

**Fig. 7** Hysteresis loop of MgFe_2O_4 nanoparticles at room temperature

are in good agreement with the literature report of pure magnesium ferrite.

3.5 Magnetic properties

The hysteresis or loop is used to determine the behavior of ferromagnetic materials when placed in the magnetic field. Figure 7 displays the room temperature hysteresis loop for MgFe_2O_4 prepared by co-precipitation method, which indicates the soft magnetic nature of the synthesized particles. The values of the saturation magnetization (M_s), coercivity (H_c), retentivity (M_r) and remanant ratio (R) were obtained from this curve as $24.520 \text{ emu g}^{-1}$, $2.9829 \text{ emu g}^{-1}$, 93.78 Oe and 0.121 respectively. The sample displayed normal (S-shaped) narrow hysteresis loop. Narrow loops indicated low coercivity value which indicates that the prepared sample can be easily demagnetized. Magnetic parameters like M_s , M_r and H_c of the samples depend upon a number of factors such as anisotropy density, grain growth and A–B exchange interactions. Smit and Wijn [35] have reported saturation magnetization value for bulk particles of MgFe_2O_4 as 27 emu g^{-1} , whereas, in the present case, the value comes out to be 24.52 emu g^{-1} . The difference in the value of saturation magnetization can be

explained on the basis of cation distribution. Any change in the concentration and nature of ions in A-and B-site causes resultant magnetization to be different from the reported one [23].

In the MgFe_2O_4 system, the magnetic properties are sensitive to the distribution of Fe^{3+} ion in A- and B-sites. It is reported [31] that the metal ion distribution in MgFe_2O_4 is given by

$$(\text{Mg}_{0.1}\text{Fe}_{0.9})_A [\text{Mg}_{0.9}\text{Fe}_{1.1}]_B$$

Its structure was originally reported to be inverted, that is, having the same number of magnetic atoms on A-sites as on B-sites [36]. On the basis of the Neel coupling model, Mg-ferrite would then be expected to have zero saturation moment. However, this was not observed experimentally and the saturation moment was found to vary within the limits of 1–2.4 Bohr magnetons depending on the conditions of preparation [37]. This discrepancy has been explained on the assumption that Mg-ferrite is incompletely inverted; the number of iron atoms on B-sites thus exceeds the number on A-sites. Smit and Wijn [35] reported the magnetic moment per molecule MgFe_2O_4 at 0 K as 1.1 Bohr magnetons. H_c of the magnetic material is a measure of its magneto-crystalline anisotropy. The value of H_c has no direct relationship with the preparation temperature and crystalline size. The lower values of magnetic parameters as compared to bulk counterparts are attributed to the smaller particle size of the ferrite NPs and existence of spin canting, which has been reported in several nanometer-sized ferrites and is dependent upon surface structural disorder [35]. It should be emphasized that surface effects can lead to a decrease or an increase in the magnetization of nanoparticles. It was reported that the magnetization of oxide nanoparticles decreases for some oxide nanoparticles [38]. On the other hand, the magnetization of some metallic nanoparticles (cobalt) was reported to increase [39]. The reduction of magnetization of oxide nanoparticles was attributed to the existence of a magnetically dead layer on the particle's surface, the existence of canted spins, or the existence of a spin-glass-like behavior of the surface spins [38].

Because of the small size of nanoparticles, large fractions of all the atoms in a nanoparticle are surface atoms [40]. Since the ratio of surface atoms to the bulk atoms is large, surface contribution to magnetization becomes significant. These surface defects result in uncompensated disordered spins at the surface of the nanoparticle leading to surface magnetization (ferromagnetism or antiferromagnetism). The surface magnetization is contributed by the surface uncompensated spins, which depend on the size of the particle and on the degree of surface disorder [41].

4 Conclusions

In this work, we report the synthesis of magnesium ferrite nanoparticle via simple and less toxic co-precipitation technique. The X-ray analysis confirmed the formation of a single-phase cubic spinel structure. FTIR result confirmed the ferrite phase formation. SEM images illustrated that the magnetic ferrite particles are formed with some agglomeration at nanoscale. The EDS results confirm the presence of the required elements in the prepared composition. The Raman result of the synthesized sample revealed the well defined Raman active modes ($A_{1g} + E_g + 3F_{2g}$) which are expected in the spinel structure and Raman spectra has a very good agreement with reported data. Furthermore, hysteresis curves obtained from magnetic measurement indicated the soft nature of the prepared nanoferrites.

Acknowledgements Authors would like to thank CSIR [No.09/013(0823)/2018-EMR-1] New Delhi for financial assistance. We are thankful to Prof. R. K. Singh, Department of Physics, Institute of Science, BHU, Varanasi for providing Raman spectra facility.

Compliance with ethical standards

Conflict of interest There is no conflict of interest among the authors.

References

- Lisjak D, Mertelj A (2018) Anisotropic magnetic nanoparticles: a review of their properties syntheses and potential applications. *Prog Mater Sci* 95:286–328
- Wang ZL, Liu Y, Zhang Z (2002) Handbook of nanophase and nanostructured materials, vol 3. Kluwer Academic/Plenum, New York
- Nonkumwong J, Pakawanit P, Wipatanawin A, Jantaratana P, Ananta S, Srisombat L (2016) Synthesis and cytotoxicity study of magnesium ferrite-gold core-shell nanoparticles. *Mater Sci Eng C* 61:123–132
- Wang G, Ma Y, Li M, Cui G, Che H, Mu J, Zhang X, Tong Y, Dong X (2017) Magnesium ferrite nanocrystal clusters for magnetorheological fluid with enhanced sedimentation stability. *Solid State Sci* 63:70–75
- Liu YL, Liu ZM, Yang Y, Yang HF, Shen GL, Yu RQ (2005) Simple synthesis of $MgFe_2O_4$ nanoparticles as gas sensing materials. *Sensors Actuators B* 107:600–604
- Kim HG, Borse PH, Jang JS, Jeong ED, Jung OS, Suhd YJ, Lee JS (2009) Fabrication of $CaFe_2O_4/MgFe_2O_4$ bulk heterojunction for enhanced visible light photocatalysis. *Chem Commun* 39:5889–5891
- Pan Y, Zhang Y, Wei X, Yuan C, Yin J, Cao D, Wang G (2013) $MgFe_2O_4$ nanoparticles as anode materials for lithium-ion batteries. *Electrochim Acta* 109:89–94
- Willey RJ, Noirclerc P, Busca G (1993) Preparation and characterization of magnesium chromite and magnesium ferrite aerogels. *Chem Eng Commun* 123:1–16
- Sivakumar N, Narayanasamy A, Greneche JM, Murugaraj R, Lee YS (2010) Electrical and magnetic behavior of nanostructured $MgFe_2O_4$ spinel ferrite. *J Alloys Compd* 504:395–402
- Hyeon T (2003) Chemical synthesis of magnetic nanoparticles. *Chem Commun* 9:927–934
- Jana NR, Chen Y, Peng X (2004) Size and shape controlled magnetic (Cr, Mn, Fe Co, Ni) oxide nanocrystals via a simple and general approach. *Chem Mater* 16:3931–3935
- Raghassudha M, Ravinder D, Veerasomaiah P (2013) Characterization of chromium substituted cobalt nano ferrites synthesized by citrate-gel auto combustion method. *Adv Mater Phys Chem* 3(2):89–99
- Dalavi SB, Mishra PP, Cherian T, Raja MM, Panda RN (2020) Magnetic and Mössbauer studies on nanostructured $CoCr_xFe_{2-x}O_4$ ($0 \leq x \leq 1$) spinel ferrites prepared by sol-gel auto-combustion method. *J Nanosci Nanotec* 20(8):983–990
- Chien YT, Yi CC, Chien ML (2018) Hydrothermally synthesized Mg-based spinel nanoferrites: phase formation and study on magnetic features and microwave characteristics. *Adv Funct Nanomater Appl* 11(11):2274
- Joshi S, Kumar M, Chhoker S, Srivastava G, Jewariya M, Singh VN (2014) Structural magnetic dielectric and optical properties of nickel ferrite nanoparticles synthesized by co-precipitation method. *J Mol Struct* 1076:55–62
- Rashad MM, Rayan DA, Turkey AO, Hessien MM (2015) Effect of Co and Y ions insertion on the microstructure development and magnetic properties of $Ni_0.5Zn_0.5Fe_2O_4$ powders synthesized using Co-precipitation method. *J Magn Magn Mater* 374:359–366
- Ningzhong B, Liming S, Yuhsiang W, Prahallad P, Arunava G (2007) A facile thermolysis route to monodisperse ferrite nanocrystals. *J Am Chem* 129(41):12374–12375
- Iqbal T, Hassan A, Ghazal S (2017) Wet chemical co-precipitation synthesis of nickel ferrite nanoparticles and their characterization. *J Inorg Organomet Poly Mater* 27:1430–1438
- Bennet J, Tholkappiyar R, Vishista K, Victor JN, Hamed F (2016) Attestation in self-propagating combustion approach of spinel AFe_2O_4 ($A = Co, Mg$ and Mn) complexes bearing mixed oxidation states: Magnetostructural properties. *Appl Surf Sci* 383:113–125
- Rashad MM, Soltan S, Ramadan AA, Bekheet MF, Rayan DA (2015) Investigation of the structural, optical and magnetic properties of $CuO/CuFe_2O_4$ nanocomposites synthesized via simple microemulsion method. *Cer Int* 41(9):12237–12245
- Liu CP, Li MW, Cui Z, Huang JR, Tian YL, Lin T, Mi WB (2007) Comparative study of magnesium ferrite nanocrystallites prepared by sol-gel and coprecipitation methods. *J Mater Sci* 42(2997):6133–6138
- Pradeep A, Priyadharsini P, Chandrasekaran G (2008) Sol-gel route of synthesis of nanoparticles of $MgFe_2O_4$ and XRD, FTIR and VSM study. *J Magn Magn Mater* 320:2774–2779
- Sivakumar N, Narayanasamy A, Greneche JM, Murugaraj R, Lee YS (2010) Electrical and magnetic behaviour of nanostructured $MgFe_2O_4$ spinel ferrite. *J Alloys Compd* 504:395–402
- Hankare PP, Jadhava SD, Sankpal UB, Patil RP, Sasikala R, Mulla IS (2009) Gas sensing properties of magnesium ferrite prepared by co-precipitation method. *J Alloys Compd* 488:270–272
- Sumangala TP, Pasqueta I, Presmanes L, Thimonta Y, Bonninguea C, Venkataramani NS, Carles VB, Tailhadesa P, Barnabé A (2018) Effect of synthesis method and morphology on the enhanced CO_2 sensing properties of magnesium ferrite $MgFe_2O_4$. *Ceramics Int* 44:18578–18584
- Nguyen LTT, Nguyen LTH, Manh NChu, Quoc DN, Quang HN, Nguyen HTT, Nguyen DC, Bach LG (2019) A facile synthesis, characterization, and photocatalytic activity of magnesium ferrite

- nanoparticles via the solution combustion method. *J Chem.* <https://doi.org/10.1155/2019/3428681>
27. Klung HP, Alexander LB (1974) *X-ray diffraction procedures.* Wiley, New York
 28. Cullity BD (1978) *Elements of X-ray diffraction.* Addison-Wesley Publishing Company Inc., Philippines
 29. Pathan AT, Mathad SN, Shaikh AM (2014) Infrared spectral studies of nanostructured Co_2 -substituted Li-Ni-Zn ferrites. *Int J Self-Propag High-Temp Synth* 23:112–117
 30. Waldron RD (1955) Infrared spectra of ferrites. *Phys Rev* 99:1727–1735
 31. Gupta R, Sood AK, Metcalf P, Honig JM (2002) Raman study of stoichiometric and Zn-doped Fe_3O_4 . *Phys Rev B* 65:1–8
 32. Gasparov LV, Tanner DB (2000) Infrared and Raman studies of the Verwey transition in Magnetite. *Phys Rev B* 62:7939–7944
 33. Pradhan DK, Mishra P, Puli VS, Sahoo S, Pradhan DK, Katiyar RS (2014) *J Appl Phys* 115:243904–243914
 34. De M, Tewari HS (2017) Structural characterization of Mg substituted on A/B sites in NiFe_2O_4 nanoparticles using autocombustion method. *J Phys* 89:1–3
 35. Smit J, Wijn HPJ (1959) *Ferrites.* Cleaver-Hume Press, London
 36. Barth TFW, Posnjak E (1932) Spinel structures: with and without variate atom equipoints, *Zeitschrift für Kristallographie* 82:325–341.
 37. Guillaud C (1951) Proprieties magnetiques des ferrites. *J Phys Le Radium* 12:239–248
 38. Kodama RH (1999) Magnetic nanoparticles. *J Magn Magn Mater* 200:359–372
 39. Respaud M, Broto JM, Rakoto H, Fert AR, Thomas L, Barbara Bet Verelst M, Snoeck E, Lecante P, Mosset A, Osuna J, Ould Ely T, Amiens C, Chaudret B (1998) Surface effects on the magnetic properties of ultrafine cobalt particles. *Phys Rev B* 57:2925–2935
 40. Batlle X, Labarta A (2002) Finite-size effects in fine particles: magnetic and transport properties. *J Phys D Appl Phys* 35:15–42
 41. Dobrynin AN, Ilev DN, Temst K, Lievens P, Margueritat J, Gonzalo J, Afonso CN, Zhou SQ, Vantomme A, Piscopiello E, van Tendeloo G (2005) Critical size for exchange bias in ferromagnetic-antiferromagnetic particles. *Appl Phys Lett* 87:01250

Publisher's Note Springer Nature remains neutral with regard to jurisdictional claims in published maps and institutional affiliations.